Chapter 33
Optimal Design and Operation of a Residential Hybrid Microgrid System in Kasuga City

Yuichiro Yoshida, Nagashima Keisuke, and Hooman Farzaneh

Abstract This study aims to find the optimal configuration of an autonomous microgrid system which can be used to meet the electricity demand of a small community in the city of Kasuga, Fukuoka Prefecture, Japan. To this aim, an optimization model was developed, using the least cost perceptive approach and the load patterns of the residential end-uses. The proposed microgrid system in this study consists of a cluster of loads and micro sources such as the wind turbines, solar photovoltaic panels, battery storage, and a diesel generator. In this research, the effect of the demand response capabilities and patterns on optimal power generation from the proposed microgrid was investigated by introducing a standard demand pattern for a family, including three residents, living in a standard Japanese house in Kasuga city.

Keywords Renewable energy · Microgrid · Energy storage · Solar · Wind · Diesel · Optimization

33.1 Introduction

After the Great East Japan Earthquake, energy security and vulnerability have become the significant challenges facing the energy system in Japan. Consequently, the rapid increase in power demand was met through higher electricity generation from fossil fuels (coal, oil, natural gas, etc.). It was associated with severe negative environmental impacts in terms of increased greenhouse gas emissions (Phurailatpam et al. 2018). Shifting to Renewable Energy Resources (RERs) can be considered as a vital solution to the problems arisen from the extensive use of fossil fuels in the electric power industry in Japan.

To promote the introduction of RERs on a large scale, following the collapse of public trust in nuclear power due to the Fukushima Daiichi nuclear disaster,

Y. Yoshida · N. Keisuke · H. Farzaneh (✉)
Interdisciplinary Graduate School of Engineering Sciences, Kyushu University, Fukuoka, Japan
e-mail: farzaneh.hooman.961@m.kyushu-u.ac.jp

H. Farzaneh
Inter/Transdisciplinary Energy Research, Kyushu University, Fukuoka, Japan

Y. Kishita et al. (eds.), *EcoDesign and Sustainability II*, Sustainable Production, Life Cycle Engineering and Management, https://doi.org/10.1007/978-981-15-6775-9_33

the government of Japan has introduced several energy resilience programs, particularly in the residential and commercial sectors in urban areas. Among all new concepts in power generation, the residential community Microgrids serve as the self-sustaining and autonomous hybrid power systems which can use a variety of RERs such as solar and wind and operate disconnected from the utility grid when outages occur. However, integrating several energy sources in microgrids also increases the complexity of the system. It is because that the main drawback of RERs is their unpredictable natures, which raises concerns about the reliability of the power to the user (Singh et al. 2016). Besides, the increasing penetration of RERs with intermittent power generation brings more significant technical challenges to maintaining the balance of power supply and demand in the power system. To this aim, diesel generators and battery storages are widely used as backup power to cover the supply and demand mismatch and improve the system stability in microgrids. However, the main disadvantages of using diesel generators with microgrid systems are their costs and environmental impacts from burning fossil fuel such as gas oil, kerosene, or fuel oil (Singh et al. 2016).

The optimal design of a microgrid in autonomous mode needs a solid understanding of the dynamic nature of the distribution network, which challenges the stability and control effectiveness of the system. In addition to the reliability of the system, the economic viability of the system plays a key role in cost-effective design and usage of a microgrid (Yoshida and Farzaneh, 2020; Shaqour et al., 2020).

Based on the above discussion, this paper will address a simulation modeling approach which can be used to estimate the optimal configuration of a proposed microgrid consisting of solar photovoltaics, wind turbines, batteries, and diesel power to meet the power demand of a selected standard Japanese house in Kasuga city in Japan. Figure 33.1 shows the overall configuration of the proposed microgrid in this research.

The optimal design of the proposed microgrid will be carried out based on finding the minimum cost of electricity generation by the system.

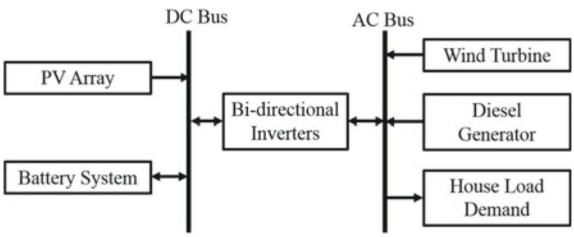

Fig. 33.1 Microgrid system

33.2 Mathematical Modeling of the Proposed System

33.2.1 Wind Power Generation

The amount of power output of a wind turbine is directly proportional to the wind speed, which can be calculated using the following formula (Dhundhara et al. 2018):

$$P_{wt}(V) = \begin{cases} \frac{P_r(V - V_{CIN})}{V_{rat} - V_{CIN}}, & V_{CIN} \le V \le V_{rat} \\ P_r, & V_{rat} \le V \le V_{CO} \\ 0, & V \le V_{CIN} \; and \; V \ge V_{CO} \end{cases} \tag{33.1}$$

where,

P_r	Constant power [kW]
V_{CIN}	Cut-in speed [m/s]
V_{rat}	Rated wind speed [m/s]
V_{CO}	Cutout speed [m/s].

$$V = V_{ref}\left(\frac{H}{H_{ref}}\right)^{\alpha} \tag{33.2}$$

V referes to the wind speed at the height of H. V_{ref} is the wind speed measured at the reference height, H_{ref}, and α, which is the power-law exponent (Hiendro et al. 2013).

$$\boldsymbol{P_{wt} = \frac{\rho}{\rho_0} P_{wt}(STP)} \tag{33.3}$$

where, $P_{wt}(STP)$ is the wind turbine power output at standard temperature and pressure [kW]. ρ shows the actual air density [kg/m^3]. ρ_0 is defined "the air density at standard temperature and pressure (1.225 kg/m^3). Table 33.1 gives the technical specifications of the Air dolphin pro wind turbine which was used in this study.

Table 33.1 Wind turbine input data (Zephyr AIRDOLPHIN Introduction. http://www.shida-kk.com/images/Airdolphin.pdf)

Constant power [kWh]	2.3
Cut-in wind speed [m/s]	2.5
Cut out wind speed [m/s]	20
Height [m]	30.5
Height of wind speed measurement (high) [m]	80
Height of wind speed measurement (low) [m]	10
Air density on sea surface [kg/m^3]	1.225

33.2.2 PV Power Generation

The amount of power output form the PV array is expressed by the following equation (HOMER 2019):

$$P_{pv} = G_{pv} f_{pv} \left(\frac{I_T}{I_{T,\,STC}} \right) [1 + \alpha_p (T_{C-} T_{C,\,STC})] \tag{33.4}$$

where,

G_{pv} Rated capacity of the PV array power, under standard test conditions [kW]
f_{pv} PV derating factor [%]
I_T Solar radiation incident on the PV array [kW/m^2]
$I_{T,STC}$ Incident radiation at standard test conditions [kW/m^2]
α_p Temperature coefficient of power [%/°C]
T_C PV cell temperature [°C]
$T_{C,STC}$ PV cell temperature under standard test conditions [25 °C].

PV cell temperature is the same as the ambient temperature at night, but it can increase during sunny days. Following equation represents the energy balance of the PV array. The input data used in this study for the simulation of the power out of a selected PV panel (Panasonic HIT 244α) is given in Table 33.2.

$$\tau \alpha G_t = \eta_c G_t + U_L (T_c - T_a) \tag{33.5}$$

where,

τ Solar transmittance the PV array [%]

Table 33.2 PV Input data (Hiendro et al. 2013) (Panasonic Residential fuel cell. http://panasonic.co.jp/ap/FC/en_index.html.)

Solar constant [kW/m^2]	1.367
Solar radiation at which the NOCT [kW/m^2]	0.8
Ambient temperature at NOCT[a] [°C]	20
NOCT [°C]	44
STC [°C]	25
Rated capacity of the PV array at STC [W/m^2]	194.44
Module efficiency (P_{max}) [%/°C]	−0.258
Slope of the surface [°]	33
Solar absorbance and the solar transmittance [%]	0.194
PV derating factor [%]	0.8
Solar absorbance and the solar transmittance [%]	0.9
Incident radiation at STC [kW/m^2]	1

[a]Nominal Operating Cell Temperature

α Solar absorptance of the PV array [%]
GT Incident solar radiation incident on the PV array [kW/m^2]
η_C Electrical conversion efficiency of the PV array [%]
U_L Overal heat transfer coefficient of the PV [$kW/m^2 °C$]
T_C PV cell temperature [°C]
T_a Ambient temperature [°C]

33.2.3 Diesel Generation

The fuel consumption of diesel generator is calculated as follows (Jamshidi and Askarzadeh 2019):

$$Cons_G = B_G \cdot P_{N\_G} + A_G \cdot P_G \tag{33.6}$$

where,

$Cons_G$ Fuel consumption of diesel generator [L/h]
P_{N_G} Nominal power of diesel generator [kW]
P_G Power output of diesel generator [kW]
A_G 0.2461 [L/kWh] and BG:0.081451 [L/kWh].

The thermal efficiency of the diesel generator is estimated by using the following equation:

$$\eta_G = \frac{P_G}{Cons_G} \tag{33.7}$$

33.2.4 Battery Modeling

In this investigation, the Kinetic Battery Model was used to determine the amount of energy that can be charged by or discharged from the storage bank in each time step. The Kinetic Battery model explains the behavior of a lead acid battery based on the operation of two storage tank. The first tank contains “available energy”, or the amount of chemical energy which is available and can be converted into DC electricity. The second tank represents “bound energy,” or energy that is chemically bound and therefore not immediately available for withdrawal. The following equations show the maximum charged by and discharged from the battery bank in each time step (Das et al. 2017):

$$Q_{1,end} = Q_1 e^{-k\Delta t} + \frac{(Qkc - P)(1 - e^{-k\Delta t})}{k} + \frac{Pc(k\Delta t - 1 + e^{-k\Delta t})}{k} \tag{33.8}$$

$$Q_{2,end} = Q_2e^{-k\Delta t} + Q(1-c)(1-e^{-k\Delta t}) + \frac{P(1-c)(k\Delta t - 1 + e^{-k\Delta t})}{k} \quad (33.9)$$

where,

Q_1	Available energy at the beginning of the time step [kWh]
Q_2	Bound energy at the beginning of the time step [kWh]
Q_{1_end}	Available energy at the end of the time step [kWh]
Q_{2_end}	the bound energy at the end of the time step [kWh]
P	Power into (positive) or out from (negative) the storage bank [kW]
Δt	Time step [h]
k	Constant coefficient which shows how quickly the storage can convert bound energy to available energy or vice versa
c	Battery capacity ratio.

The total amount of energy stored in the battery bank at each time step is the sum of the available energy and bound energy:

$$Q = Q_1 + Q_2 \quad (33.10)$$

The battery state of charge (SOC) is given as follows, whereby Q_{max} is the maximum (rated) capacity of the battery bank:

$$SOC = \frac{Q}{Q_{max}} \times 100(\%) \quad (33.11)$$

The following equation gives the maximum amount of power charged by ($P_{Maxchar}$) and discharged ($P_{Maxdiscahr}$) from the battery bank which can be absorbed over a specific length of time (Δt) (Table 33.3):

$$P_{Maxchar} = \frac{kQ_1e^{-k\Delta t} + Qkc(1-e^{-k\Delta t})}{1-e^{-k\Delta t} + c(k\Delta t - 1 + e^{-k\Delta t})} \quad (33.12)$$

$$P_{Maxdischar} = \frac{-kcQ_{max} + kQ_1e^{-k\Delta t} + Qkc(1-e^{-k\Delta t})}{1-e^{-k\Delta t} + c(k\Delta t - 1 + e^{-k\Delta t})} \quad (33.13)$$

33.3 Optimization

33.3.1 Cost Analysis

In this study, the Levelized Cost of Energy (LCOE) was considered as a measure for comparative analysis of various power generation technologies (i.e. solar, wind, and

Table 33.3 Battery input data (Dhundhara et al. 2018)

Battery Type	Lead-acid
Nominal cell voltage (V)	12
Nominal cell maximum capacity (Ah)	83.4
Nominal capacity (kWh)	1
Cycle life @ maximum DOD	800
DoD (20–80%)	0.60
Float life	4
Round-trip efficiency (%)	80
Battery rate constant (2.12 h^{-1})	2.12
Battery capacity ratio	0.305
Amount of available charge in the beginning (Ah)	25.43
Storage's maximum charge current (A)	10
Maximum storage bank charge power corresponding to maximum charge current (Ah/Kwh)	0.48
Charging efficiency (%)	85
Discharge efficiency (%)	100
k : Constant coefficient of battery	0.45

diesel) in the proposed microgrid. The LCOE represents the net present value of the total cost of the microgrid over its lifetime, divided by the total output power from the system (DOE Office of Indian Energy Upfront Capital Costs for Renewables.,https://www.energy.gov/sites/prod/files/ 2015):

$$LCOE = \frac{S_{CL}}{S_{EL}} = \frac{\sum_{i=1}^{n} \frac{I_t + M_t + F_t}{(1+r)^t}}{\sum_{i=1}^{n} \frac{E_t}{(1+r)^t}} \tag{33.14}$$

where,

S_{CL} Sum of costs over the lifetime ($)
S_{EL} Sum of electrical energy produced over the lifetime (kWh)
I_t Investment expenditures in the year t ($)
M_t O&M expenditures in the year t ($)
F_t Fuel expenditures in the year t ($)
E_t Electrical energy generated in the year t (kWh)
r Discount rate (%)
n Expected lifetime of system or power station.

For the battery storage, the following formula may be used to compute the LCOE (What is the true cost to you behind energy storage?,https://www.solarpowerworldonline.com/ 2016):

$$LCOE_{battery} = \frac{P}{C_a \times C_y \times E_f \times DoD} + T_{AC} \tag{33.15}$$

where,

P Price of the battery storage ($)
C_y Number of full charge and discharge cycles expected over the guaranteed life of the battery
C_a Capacity of the battery storage (kWh)
E_f Storage efficiency (%)
DoD Depth of discharge (%)
T_{AC} Total ancillary costs ($).

The cost items, including the capital investment, and operation costs of the main components of the proposed microgrid is given in Table 33.4. Based on these values, the LCOE for each component is derived and is shown in Table 33.5.

Table 33.4 Cost items of each component

Cost Item	Battery (Das et al. 2017)	Wind (Zephyr AIRDOLPHIN Introduction. http://www.shida-kk.com/images/Airdolphin.pdf)	PV (Panasonic Residential fuel cell. http://panasonic.co.jp/ap/FC/en_index.html.)	Diesel (Jamshidi and Askarzadeh 2019)
Capital cost(JPY/KW)	13,600	300,000	730,000	60,000
O&M Cost[1] (JPY/kWh)	1100	1500	3600	130
Life time (years)	4	20	20	3

1. Including the fuel cost

Table 33.5 LCOE for each component

	PV	Wind	Batterty	Diesel
Rated output [kWh/unit]	0.24 (Panasonic Residential fuel cell. http://panasonic.co.jp/ap/FC/en_index.html.)	2.3 (Zephyr AIRDOLPHIN Introduction. http://www.shida-kk.com/images/Airdolphin.pdf)	1	1.9
LCOE [yen/kWh]	40.0	22.4	91.1	151.2

33.3.2 Optimization Model

The objective function of the optimization model is defined as the total cost of electricity supplied by the proposed system as follows (Farzaneh, 2019):

$$Total\ energy\ cost = \sum_{t} \sum_{e} Cost_{e,t} \tag{33.16}$$

where,

$Cost_{e,t}$: the cost of using of each component e $\in [PV, Wind, Battery, Diesel]$ at each hour t ($0 \leq t \leq 23$).

In the above equation, the cost of electricity generated by each component is calculated as follows:

$$Cost_{e,t} = LCOE_e.E_{e,t} \tag{33.17}$$

where,

$LCOE_e$ LCOE of component e,
$E_{e,t}$ Amount of electricity generated by component e in time step t

The cost function is minimized subject to the following constraints:

$$E_{PV,t} + E_{Wind,t} + E_{Battery\_discharge,t} + E_{Diesel,t} \geq E_{Demand,t} \tag{33.18}$$

$$E_{Battey\_Charge,t} = E_{PV,t} + E_{Wind,t} - E_{Demand,t} \tag{33.19}$$

$$E_{Battery,charge,t} \leq P_{Maxchar}.\Delta t \tag{33.20}$$

$$E_{Battery,discharge,t} \leq P_{Maxdischar}.\Delta t \tag{33.21}$$

$$0.2 \leq SOC \leq 0.8 \tag{33.22}$$

$$E_{Diesel,\mathrm{t}} \leq C_{load} P_{Diesel} \tag{33.23}$$

where,

C_{load} The load factor for emergency diesel usage, which is set to 0.7.
$E_{Demand,t}$ Amount of electricty demand at hour t

33.4 Results and Discussions

In this research, a standard demand pattern, so-called “Normal schedule” was considered as the baseline load for a Japanese family, including three residents (Father, Mother, and a kid), living in an average size house (94.13 m^2, 4 rooms) located in Kasuga city, Fukuoka prefecture. The usage method of the main electrical appliances in the normal schedule is shown in Table 33.6. The rated electrical power of each appliance is given in Table 33.7. Accordingly, the load curve in the Normal schedule based on a daily average electricity demand in the selected case study is illustrated in Fig. 33.2. The total amount of electricity demand calculated here was roughly in agreement with the average Japanese household electricity demand based

Table 33.6 Usage schedule

Normal schedule				
Hour	AC	Refregirator	TV	Light
0:00	OFF	ON	OFF	OFF
1:00	OFF	ON	OFF	OFF
2:00	OFF	ON	OFF	OFF
3:00	OFF	ON	OFF	OFF
4:00	OFF	ON	OFF	OFF
5:00	OFF	ON	OFF	OFF
6:00	OFF	ON	OFF	OFF
7:00	OFF	ON	ON	OFF
8:00	ON	ON	ON	ON
9:00	ON	ON	OFF	ON
10:00	ON	ON	OFF	ON
11:00	ON	ON	OFF	ON
12:00	ON	ON	OFF	ON
13:00	ON	ON	OFF	OFF
14:00	OFF	ON	OFF	OFF
15:00	OFF	ON	OFF	OFF
16:00	OFF	ON	OFF	ON
17:00	ON	ON	ON	ON
18:00	ON	ON	ON	ON
19:00	ON	ON	ON	ON
20:00	ON	ON	ON	ON
21:00	ON	ON	ON	ON
22:00	ON	ON	ON	ON
23:00	OFF	ON	ON	ON

Table 33.7 Electric appliances rated power

Electric appliances	Power consumption [kW]	
TV	0.057	
Refrigerator	0.228	
Lighting	0.0358	
Air conditioner (AC)	0.815 (Cooling)	0.957 (Heating)

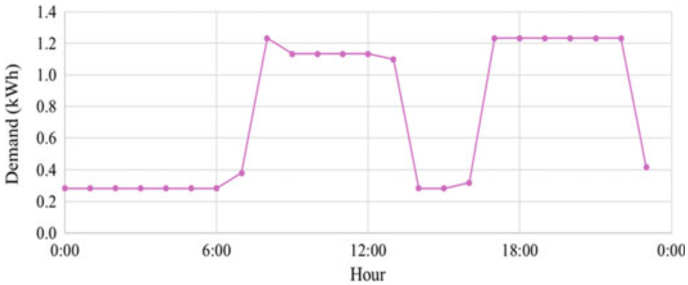

Fig. 33.2 Hourly average demand load curve

on collected data from the agency for Natural Resources and Energy in Japan [Annual Report on Energy (White Paper 2013)].

The developed model was used to estimate the optimum size and capacity of the proposed microgrid system. The optimum configuration of the microgrid comprises a system with a 2.3 kW of the wind turbine, 4.3 kW of the PV panels, six units of 1kWh batteries and 0.5 kW of diesel generator. Based on the results of the optimization model, the hourly electricity supplied by the proposed microgrid in summer and winter is depicted in Fig. 33.3.

Figure 33.4 shows the monthly average electricity supplied by the proposed microgrid. The diesel generator is only used in summer due to lack of availability of wind energy.

Figure 33.5 shows that the battery bank accounts for 50 and 64% of the total cost of electricity generation in summer and winter, respectively.

The modeled LCOE is compared to the existing tariff structure in Japan in Fig. 33.6. The estimated LCOE's of the proposed microgrid is on the order of 64.7 JPY/kWh in summer and 51.26 JPY/kWh in winter which is still well above the average electricity tariff in Japan, creating a cost gap that should be addressed through effective policy and incentive programs in the near future.

33.5 Conclusion

In this paper, modeling and simulation of a fully autonomous microgrid system were conducted in order to find the optimal configuration of the system based on the minimum total cost of the electricity generation. The representative micro-grid

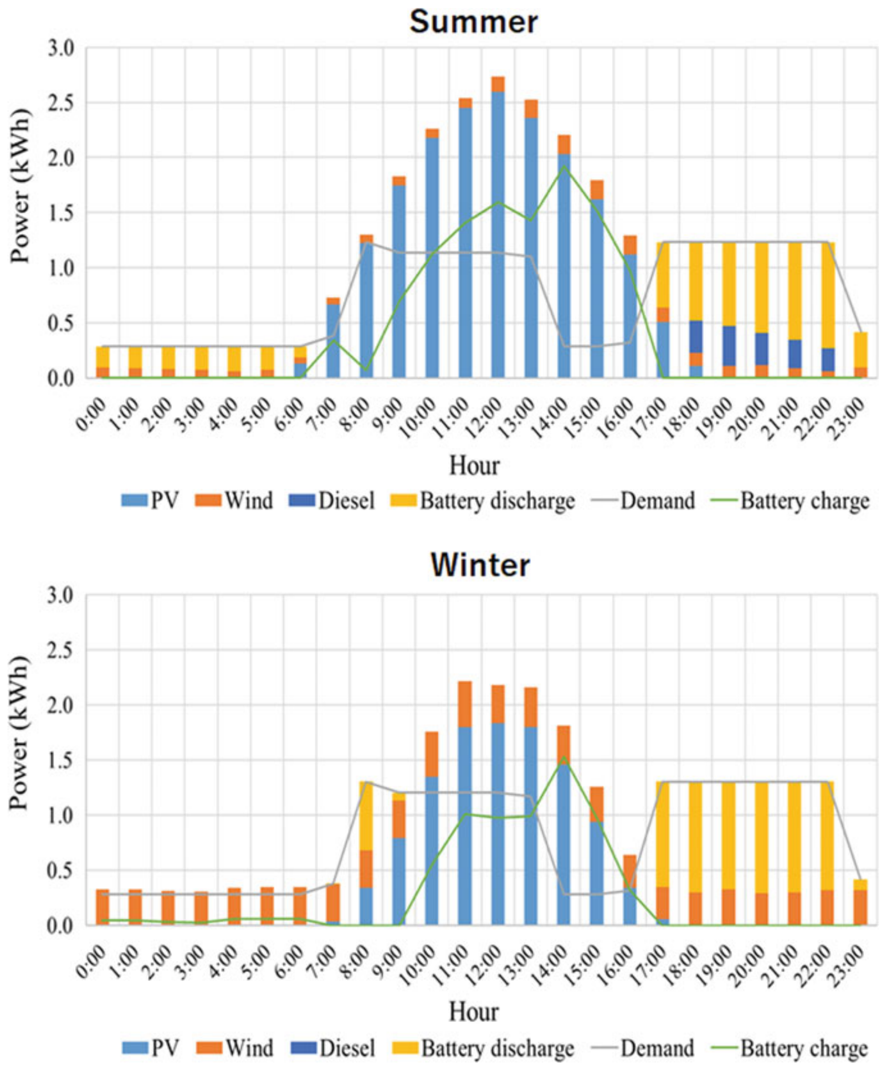

Fig. 33.3 Hourly electricity generation from the proposed microgrid

system considered includes a hybrid solar-wind-battery-diesel generation system, which currently is the most widely applicable and rapidly growing microgrid system type. The proposed microgrid was planned to be analyzed in a standard Japanese house in Kasuga city in Fukuoka prefecture. The results revealed the total power output from the system could sufficiently meet the demand load requirements of the selected household area. This simple analysis offered an estimate of the gap between current tariff regime in Japan and the LCOE of the system which can provide

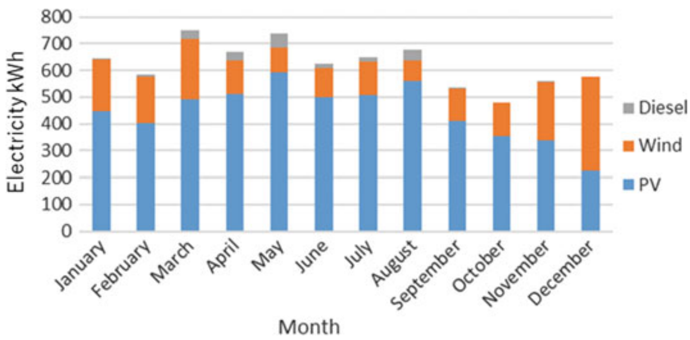

Fig. 33.4 Monthly electricity generation

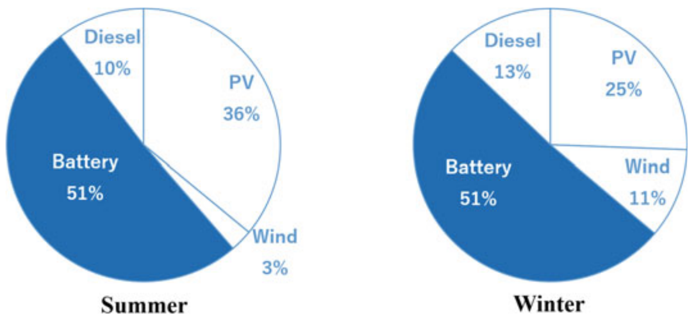

Fig. 33.5 Share of the different components in total electricity generation cost

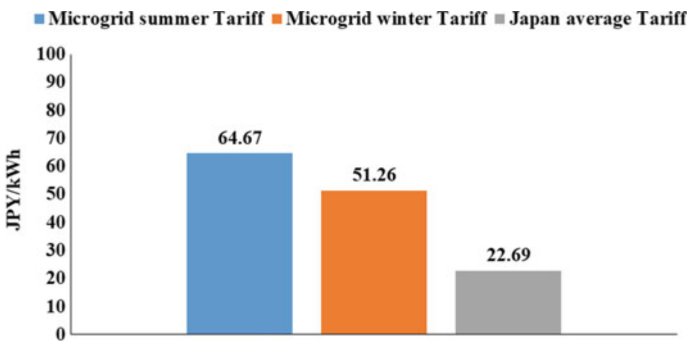

Fig. 33.6 The LCOE comparison

insight into the potential scale of incentives that may be required to enable micro-grid development under the current regulatory structure.

References

Annual Report on Energy (Energy White Paper 2013) Agency Nat. Resour. Energy. https://www.enecho.meti.go.jp/about/whitepaper/2013pdf/

Das BK, Hoque N, Mandal S, Pal TK, Raihan MA (2017) A techno-economic feasibility of a stand-alone hybrid power generation for remote area application in Bangladesh. 134:775–788

Dhundhara S, Verma YP, Williams A (2018) Techno-economic analysis of the lithium-ion and lead-acid battery in microgrid systems. Energy Convers Manag 177:122–142

DOE Office of Indian Energy Upfront Capital Costs for Renewables.,https://www.energy.gov/sites/prod/files/2015/08/f25/LCOE.pdf

Farzaneh H (2019) Energy systems modeling: principles and applications. ISBN: 978-981-13-6220-0, Springer

Hiendro A, Kurnianto R, Rajagukguk M, Simanjuntak YM, Junaidi (2013) Techno-economic analysis of photovoltaic/wind hybrid system for onshore/remote area in Indonesia 59:652–657

HOMER (2019) HOMER Pro 3.11. https://www.homerenergy.com/products/pro/docs/3.12/index.html

Jamshidi M, Askarzadeh A (2019) Techno-economic analysis and size optimization of an off-grid hybrid photovoltaic, fuel cell and diesel generator system. Sustain Cities Soc 44:310–320

Panasonic Residential fuel cell. http://panasonic.co.jp/ap/FC/en_index.html

Phurailatpam C, Rajpurohit BS, Wang L (2018) Planning and optimization of autonomous DC microgrids for rural and urban applications in India. Renew Sustain Energy Rev 82:194–204

Shaqour A, Farzaneh H, Yoshida Y, Tatsuya H (2020) Power control and simulation of a building integrated stand-alone hybrid PV-wind-battery system in Kasuga City, Japan, Energ Rep 6:1528–1544

Singh S, Singh M, Kaushik SC (2016) Feasibility study of an islanded microgrid in rural area consisting of PV, wind, biomass and battery energy storage system. Energy Convers Manag 128:178–190

What is the true cost to you behind energy storage?,https://www.solarpowerworldonline.com/2016/12/calculating-true-cost-energy-storage/

Yoshida Y, Farzaneh H (2020) Optimal design of a stand-alone residential hybrid Microgrid system for enhancing renewable energy deployment in Japan. Energ 13(7):1737

Zephyr AIRDOLPHIN Introduction. http://www.shida-kk.com/images/Airdolphin.pdf